Polymer 50 (2009) 218–226

Contents lists available at ScienceDirect

Polymer

journal homepage: www.elsevier.com/locate/polymer

POSS grafting on PPgMA by one-step reactive blending

Alberto Fina [a,*], Daniela Tabuani [a], Ton Peijs [b], Giovanni Camino [a]

[a] Politecnico di Torino, Centro di Cultura per l'Ingegneria delle Materie Plastiche, INSTM Local Research Unit, V.le T. Michel, 5, 15100 Alessandria, Italy
[b] Queen Mary, University of London, Department of Materials, Mile End Road, E1 4NS London, United Kingdom

ARTICLE INFO

Article history:
Received 18 September 2008
Received in revised form
31 October 2008
Accepted 1 November 2008
Available online 8 November 2008

Keywords:
POSS
Reactive blending
Maleic anhydride-grafted polypropylene

ABSTRACT

This paper reports the preparation of maleic anhydride-grafted polypropylene (PPgMA)/Polyhedral Oligomeric SilSesquioxanes (POSS) hybrids by POSS grafting during a one-step reactive blending process. The morphology of the hybrid was studied in details by means of electronic microscopy (SEM, TEM) as well as by X-ray diffraction, showing POSS dispersion at the nanoscale. The grafting yield, assessed through extraction of non-grafted POSS showed a high efficiency of the reactive blending process. Thermal, rheological and mechanical properties were studied for POSS-grafted PPgMA in comparison with a non-reactive PPgMA/POSS nanocomposite as a reference and showed advantages in terms of higher thermal stability and improved mechanical properties in the case of the grafting process with respect to simple melt blending.

1. Introduction

The modification of polymer chemical structure by grafting new chemical species on the polymer backbone is a very appealing way to give new or improved properties to the resulting materials. This approach has been largely used for the compatibilisation of immiscible polymer blends [1,2] and for the preparation of functional polymers [3,4]. Different techniques have been developed, including processes initiated by chemical reactions, irradiation techniques, photochemical and plasma induced grafting [3].

Concerning polypropylene modification, free radical grafting processes have been widely studied in order to obtain functionalisation with various organic groups including maleic anhydride, acrylic, methacrylic and vinyl species [4–7].

Maleic anhydride-grafted polypropylene (PPgMA) is an easily modifiable system, owing to the presence of MA groups along PP backbone. The reactivity of PPgMA with model amine species (hexamethylene diamine) in the molten state has been recently assessed, showing quantitative conversion to imide [8].

Polyhedral Oligomeric SilSesquioxanes (POSS) are organic/inorganic molecules with general formula $(RSiO_{1.5})_n$ where R is hydrogen or an organic group, such as alkyl, aryl or any of their derivatives [9–11]. Because of their size (approx. 1–3 nm), POSS can be used to modify properties of organic polymers at the molecular level. Moreover, their tailorable and well defined structure makes POSS versatile nano-building blocks in the preparation of organic/inorganic hybrid materials [12–14].

Despite the fact that in situ copolymerisation of POSS to produce hybrid organic/inorganic polymers with pendent POSS groups has been widely studied for both thermoplastics and thermosets [15–18], showing improved thermal and physical properties, POSS reactive blending is still in its infancy. Zhou et al. reported the reactive blending preparation of polypropylene/octavinyl POSS by free radical reaction, showing PP gelation [19]. To the best of the authors' knowledge, the present paper reports the first attempt to produce a polymer hybrid through monofunctional POSS grafting by melt blending. Indeed, the possibility to take advantage of the amino-anhydride reaction to produce a polymer–POSS hybrid by one-step reactive melt blending is explored. The principle reaction which is at the basis of this work is reported in Scheme 1. The correspondent nanocomposite prepared with unreactive POSS is addressed for comparison.

2. Experimental section

2.1. Materials

Octaisobutyl POSS (oib-POSS) and aminoethylaminopropyl heptaisobutyl POSS (am-POSS) were purchased from Hybrid Plastics (USA)[1] as crystalline powders and used as received. Chemical structures for oib-POSS ($M = 873.6$ g/mol) and am-POSS ($M = 917.6$ g/mol) are reported in Fig. 1.

* Corresponding author. Tel.: +39 0131 229316; fax: +39 0131 229331.
E-mail address: alberto.fina@polito.it (A. Fina).

[1] Catalog available at www.hybridplastics.com.

0032-3861/$ – see front matter © 2008 Elsevier Ltd. All rights reserved.
doi:10.1016/j.polymer.2008.11.002

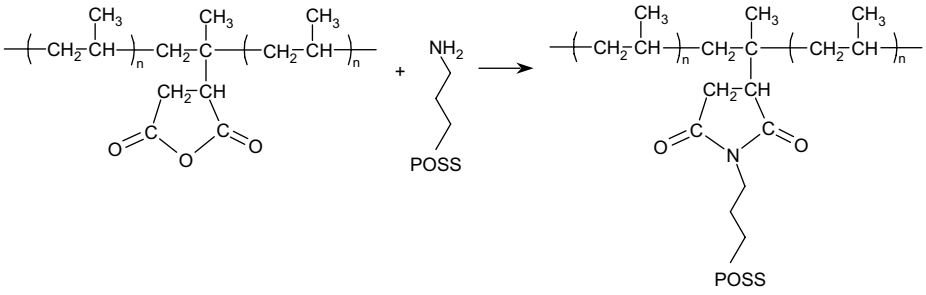

Scheme 1. Reaction between PPgMA and amino POSS producing imide bond.

PPgMA was a Polybond 3200 from Crompton Corp. (USA), containing 1%wt. of MA functions[2]. PPgMA/POSS nanocomposite and hybrid were prepared mixing PPgMA and POSS at 5%wt. in a Brabender internal mixer W50E (180 °C, 10 min, 60 rpm), accordingly with previously reported processing conditions [20,21]. Neat PPgMA was processed and characterised under the same conditions as the reference material.

Reactive POSS loading was calculated in order to obtain a molar ratio [maleic anhydride]/[amine] equal to 2:1. This ratio has been chosen considering that amine–PPgMA reactions in the melt show complete conversion only in defective amine concentrations [8] as well as taking into account the possible presence in the commercial PPgMA of a fraction of unbound anhydride, which is subject to volatilisation during compounding. It is worth noticing that this POSS loading corresponds to a very low molar concentration, roughly accounting for one POSS molecule per 400 propylene units. The same POSS loading was used in the case of unreactive POSS for comparison.

2.2. Characterisation

Scanning Electron Microscopy (SEM) micrographs were obtained by means of a LEO 1450 VP instrument equipped with a back scattered electron detector. Samples were prepared by cryogenic fracture to observe a representative section of the materials, avoiding plastic deformation.

Transmission electron microscopy (TEM) analyses were performed with high-resolution equipment (JEOL 2010). Ultrathin sections of about 100 nm thick were cut with a Power TOMEX microtome equipped with a diamond knife and placed on a 200-mesh copper grid and stained with ruthenium tetraoxide to obtain sufficient phase contrast.

X-Ray diffraction (XRD) patterns were obtained on a Thermo ARL XTRA48 diffractometer using Cu Kα radiation ($\lambda = 1.54062$ Å).

Differential Scanning Calorimetry (DSC) analyses were run using a TA Q1000 instrument in hermetic aluminium pans, under nitrogen flow (50 ml/min). Tests were performed at 10 °C/min heating rate, from 30 to 190 °C, with *ca.* 5 mg samples taken from the injection moulded specimens for tensile tests. Degree of crystallinity (X_c) was calculated from the ratio $\Delta H/\Delta H_0$, with $\Delta H_0 = 189$ J/g for PP [22] and ΔH the melt enthalpy, normalised on the actual PPgMA fraction in the formulation.

Thermogravimetry (TGA) was performed on a TA Q 500 instrument, on *ca.* 10 mg samples, in Platinum pans, with gas flows of 60 ml/min for sweeping gas (nitrogen or air), and 40 ml/min for balance protection gas (nitrogen) on heating at 10 °C/min, between 50 and 600 °C or in isothermal conditions.

In the following, T_{onset} is defined as the temperature corresponding to 5% mass loss and T_{max} is the temperature for maximum mass loss rate.

Rheological tests were performed on a strain-controlled rheometer ARES (TA Instruments) equipped with a forced air convection oven and parallel plate geometry ($R = 12.5$ mm). All the measurements were conducted under nitrogen atmosphere at a temperature of 170 °C.

ASTM standard [23] specimens for tensile tests (type V, 1 mm thickness, 63 mm length) were prepared on a Babyplast 6/10 injection moulding machine by Cronoplast. Tensile tests were performed on an Instron 5584 dynamometer, with a 1 kN load cell, at 10 mm/min with no preload applied, using a 12.5 mm Instron "clip-on" extensometer placed on the linear part of the specimen. Five tests were performed on each material; average values are reported here with their deviation from the average.

Dynamic Mechanical Thermal Analysis (DMTA) was performed on a TA Q 800 instrument in tensile mode at an oscillatory frequency of 1 Hz with applied deformation of 15 μm and 0.4 N preload. Temperature scans between −80 and 140 °C were performed at 2 °C/min heating rate. The central part of the tensile dog-bone specimens (ASTM D638 type V) was used for DMTA measurements, with 25 mm between the grips. Due to the dog-bone shape, the specimen cross-section is not constant between grips: the dimension of the narrow section was used for calculations and the obtained moduli are not intended as absolute values and will only be used for comparison between the different formulations discussed in this paper.

Purification from unreacted POSS was obtained by solubilisation of 1.5 g of PPgMA/POSS in 15 ml of boiling xylene, followed by precipitation in 150 ml cold chloroform, this being a good solvent for POSS and a non-solvent for PP. The collected precipitate was

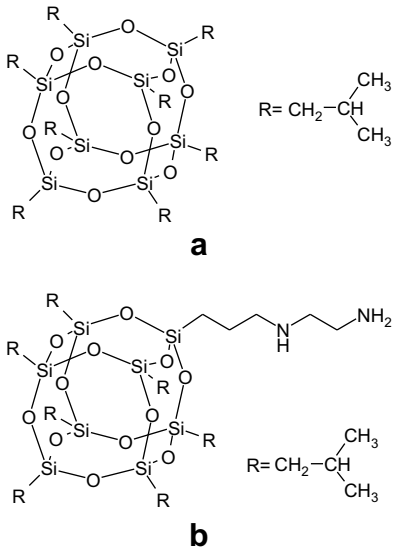

Fig. 1. Chemical structures for oib-POSS (a) and am-POSS (b).

[2] From product datasheet available at www.cromptoncorp.com.

then washed with chloroform and finally dried to remove all solvents.

Transmission FTIR spectra (resolution 4 cm^{-1}) were recorded on a Perkin–Elmer Spectrum GXIII spectrophotometer. FTIR spectra were subtracted of the baseline and normalised on the PP $\gamma_r(CH_2)$, $\delta(CH) + \gamma_r(CH_3)$) band at 899 cm^{-1} [24]. The normalised FTIR absorptions on the POSS ν(Si–O–Si) stretching band at *ca.* 1119 cm^{-1} were used to determine the POSS grafting yield, defined as the ratio between absorption peak after purification and absorption peak before purification.

Size exclusion chromatography (SEC) was performed at 145 °C on a Waters GPCV2000 instrument, equipped with Polymer Laboratories 3 PLgel Olexis columns and a differential refractive index detector. Samples were prepared in *o*-dichlorobenzene solution (2 mg/ml), in presence of ionol (0.05%) as an antioxidant, and calibration was performed with polystyrene standards (from 5,480,000 to 162 g/mol).

3. Results and discussion

3.1. Morphology

Morphological characterisation was performed by means of SEM, TEM and XRD measurements. In Fig. 2, SEM micrographs for PPgMA/oib-POSS and PPgMA/am-POSS are reported. It can be clearly seen that in the case of PPgMA/oib-POSS (Fig. 2a) residual micron-sized POSS aggregates are present in the polymer matrix, as evidenced by EDS analyses, similarly to what already was observed for a PP/oib-POSS system [20]. Conversely, no micron size aggregates can be detected in the PPgMA/am-POSS sample, evidencing a fully homogeneous microstructure.

Morphology at the nanoscale was investigated by means of TEM, taking several micrographs in different sampling points; representative images are reported in Fig. 3. PPgMA/oib-POSS micrographs show residual submicronic POSS monocrystals with regular cubic shape, as reported in Fig. 3a. A different nanostructure is observed in PPgMA/am-POSS, with the presence of rounded POSS-rich zones, as confirmed by EDS analysis, and no large (e.g. 100 nm) POSS monocrystals were detected (Fig. 3b).

Given the crystallinity of am-POSS, the aggregation of POSS moieties into irregular clusters suggests that constraints apply on POSS, possibly due to POSS grafting on PPgMA chains, hindering the regular packing into large crystals of regular shape.

The presence of POSS crystals in PPgMA, as well as the effects of POSS on PPgMA crystallinity, was studied by means of XRD analysis. Diffraction patterns for oib-POSS, PPgMA and PPgMA/oib-POSS are reported in Fig. 4. oib-POSS presents several sharp diffraction peaks due to its high crystallinity; in particular, peaks at 8.0° and 8.8° 2θ angle are the most intense. PPgMA shows the typical XRD pattern for α-PP crystallographic form, with main peaks at 14.1° (110), 16.9° (040), 18.6° (130), 21.1° (111) and 21.8° (041) [25,26]. The XRD pattern for PPgMA/oib-POSS is very similar to neat PPgMA,

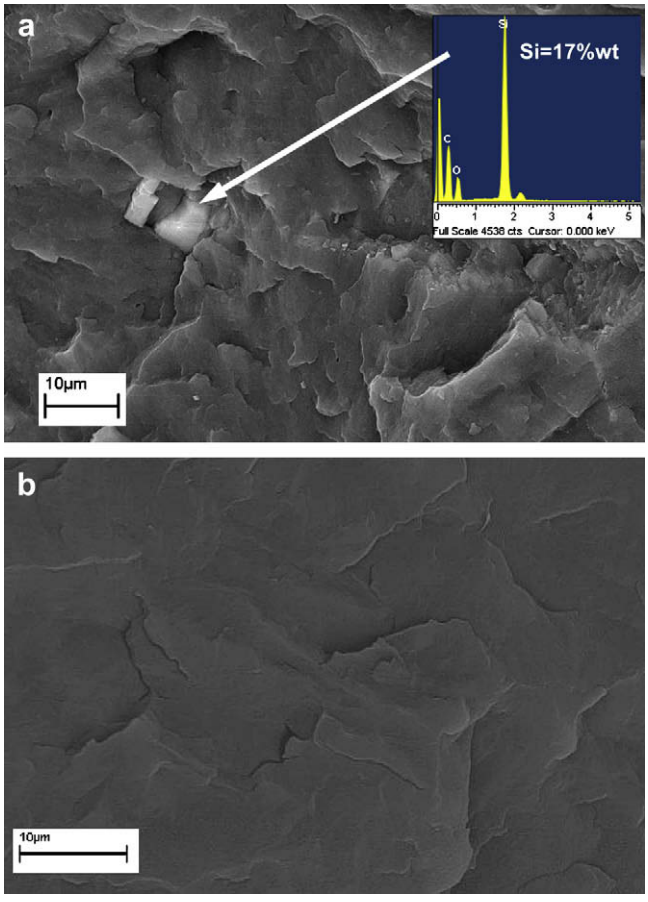

Fig. 2. SEM micrographs of PPgMA/oib-POSS with EDS elemental analysis inset (a) and SEM micrograph of PPgMA/am-POSS (b).

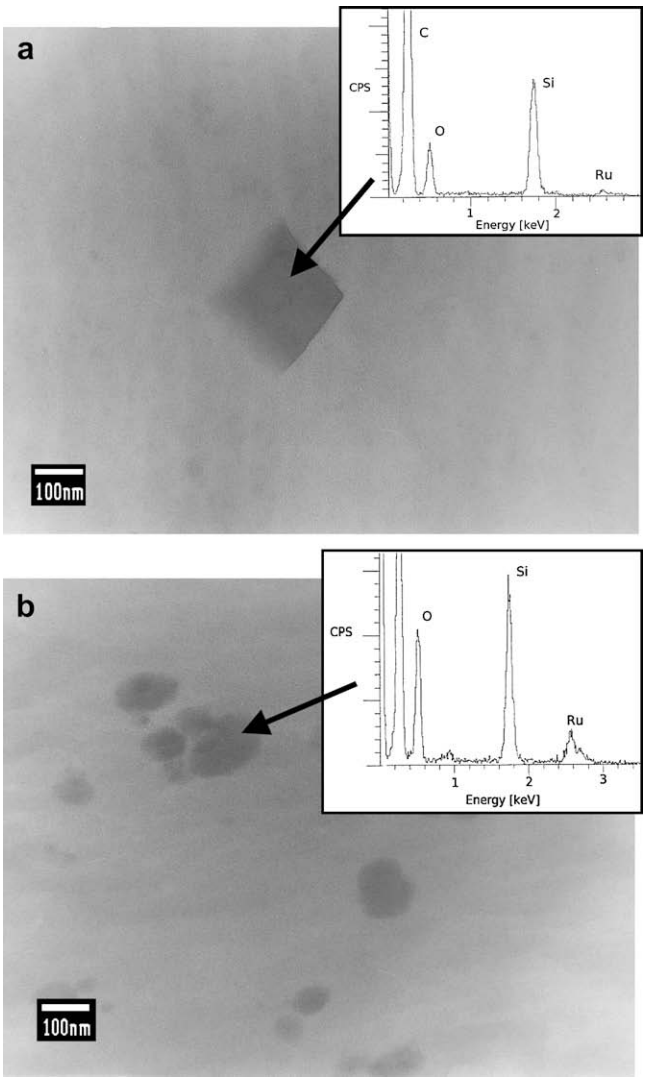

Fig. 3. TEM micrographs and EDS elemental analyses (inset) of PPgMA/oib-POSS (a) and PPgMA/am-POSS (b).

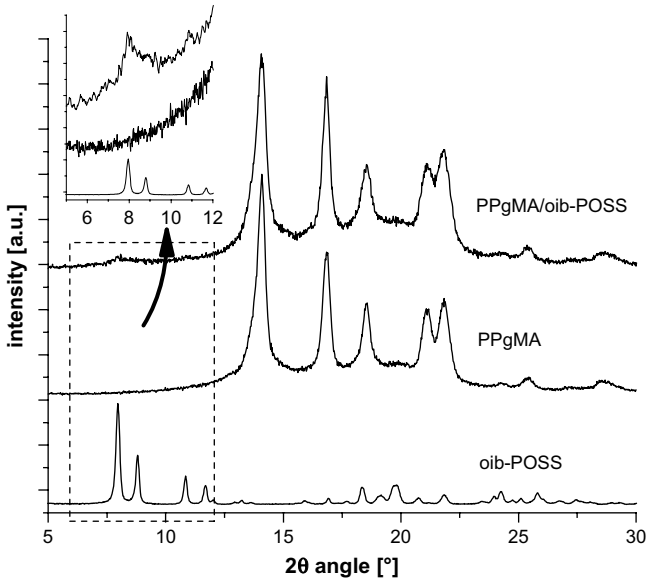

Fig. 4. XRD patterns for oib-POSS, PPgMA and PPgMA/oib-POSS (curves shifted for clarity).

showing the α-PP signals described above. In the low 2θ angle range (6–12°) signals corresponding to the POSS main diffraction peaks are observable, confirming the presence of residual POSS crystals in the PPgMA matrix.

XRD patterns for am-POSS and PPgMA/am-POSS are reported in Fig. 5, compared to the above described diffractogram for PPgMA. am-POSS shows the highest intensity diffraction peak at 8.3° 2θ angle, together with other lower intensity peaks at higher angles. PPgMA/am-POSS also crystallises in PP α form; studying in details the range 6–11° 2θ angle, a very weak and broad band is observed for PPgMA/am-POSS, which is compatible with the presence of nanoscale POSS clusters.

3.2. Grafting yield

In order to study the grafting yield, compounds obtained by melt blending were purified from non-grafted POSS following the method as described in Section 2 and the obtained materials were studied by FTIR spectroscopy.

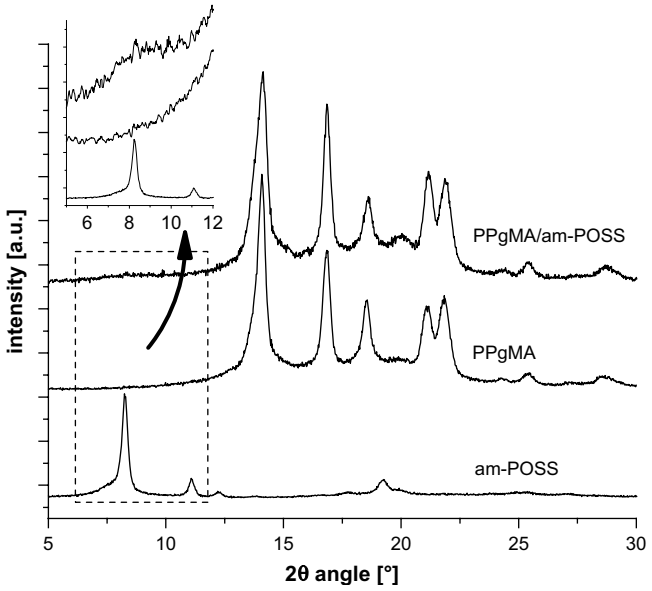

Fig. 5. XRD patterns for am-POSS, PPgMA and PPgMA/am-POSS (curves shifted for clarity).

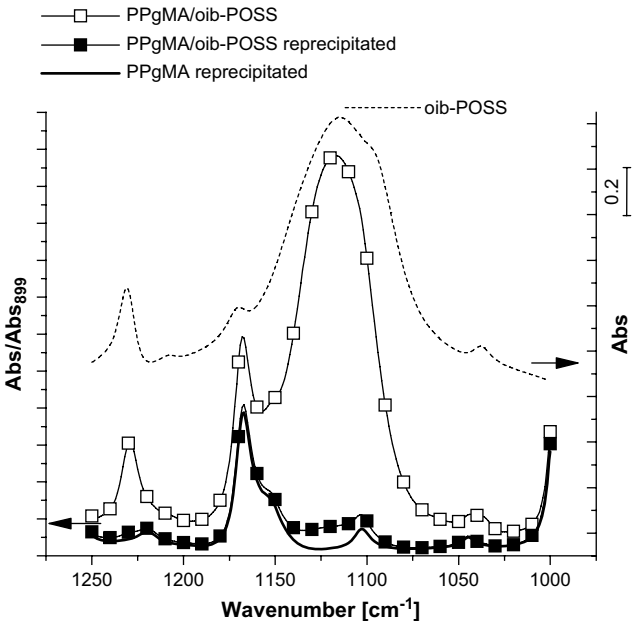

Fig. 6. Normalised FTIR spectra for PPgMA/oib-POSS before and after reprecipitation, compared to reprecipitated PPgMA and oib-POSS.

Purification from non-grafted POSS was first performed on PPgMA and PPgMA/oib-POSS to validate the extraction method. In Fig. 6, the efficiency of the purification method is clearly evidenced by the disappearance of the Si–O–Si stretching signal at 1119 cm^{-1} in the PPgMA/oib-POSS sample after extraction, compared to the same material as obtained from melt blending.

In Fig. 7, normalised FTIR spectra for PPgMA/am-POSS before and after purification from ungrafted POSS are shown, compared to reprecipitated PPgMA and am-POSS. Based on this result, grafting yield calculated from the intensities of the Si–O–Si absorption signal is 74%, evidencing that most of the amino POSS is chemically bonded to PPgMA chains after the one-step reactive blending process.

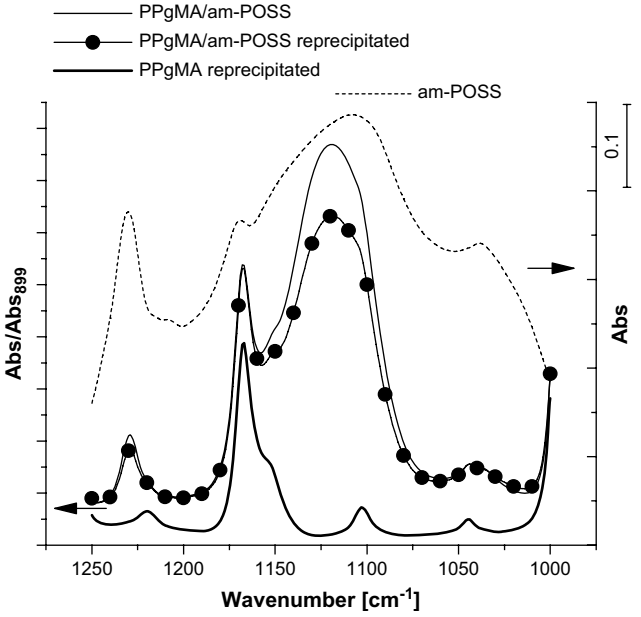

Fig. 7. Normalised FTIR spectra for PPgMA/am-POSS before and after reprecipitation, compared to reprecipitated PPgMA and am-POSS.

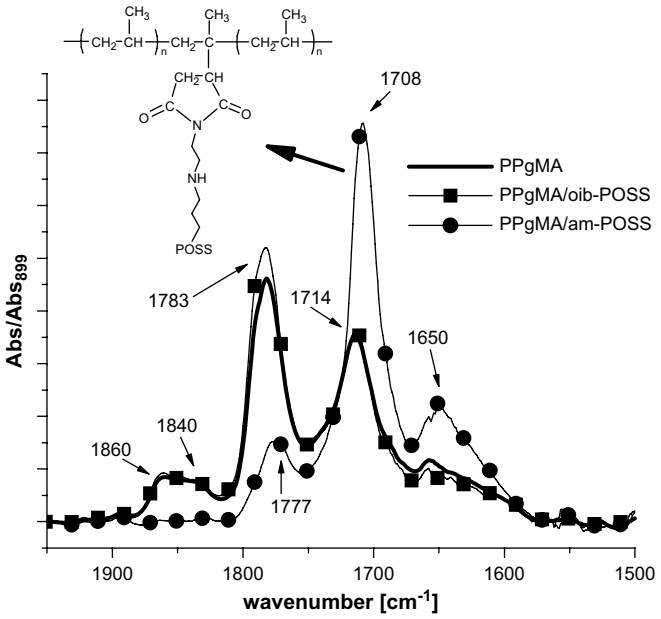

Fig. 8. Normalised FTIR spectra in the range of C=O absorptions for PPgMA, PPgMA/oib-POSS and PPgMA/am-POSS as obtained by melt blending. Neither oib-POSS nor am-POSS shows significant absorption band in this spectral region.

Further evidence for the grafting reaction as well as insights in the reaction products is obtained from the study of the carbonyl band through FTIR. Spectra acquired on PPgMA, PPgMA/oib-POSS and PPgMA/am-POSS as obtained after melt blending are reported in Fig. 8.

Several absorption bands are shown in PPgMA spectrum in the range from 1550 to 1900 cm^{-1}. Signals centred at *ca.* 1840 and 1860 cm^{-1} are assigned to asymmetric stretching of anhydride carbonyl groups, whereas the major bands centred at 1783 and 1714 cm^{-1} correspond to anhydride symmetric carbonyl groups and to carboxylic groups stretching respectively (Fig. 8).

The spectrum for PPgMA/oib-POSS does not show significant differences as compared to the reference polymer matrix, indicating that no changes in the molecular structure of PPgMA are brought by blending with oib-POSS.

Conversely, the comparison of spectra for PPgMA and PPgMA/am-POSS points out significant modification of the FTIR absorptions in the carbonyl region, which implies that a reaction has occurred on the MA groups upon blending. Indeed, both peaks at 1840 and 1860 cm^{-1} disappear and the peak at 1783 cm^{-1} decreases strongly in intensity and shifts to lower wave numbers in PPgMA/am-POSS. On the other hand, a strong peak at 1708 cm^{-1} appears. These findings suggest the occurring of a reaction between MA groups with the formation of imide groups (peaks at 1708 and 1777 cm^{-1}), in agreement with assignments in Ref. [8].

Moreover, an intensity increase of the absorption band centred at *ca.* 1650 cm^{-1} in PPgMA/am-POSS compared to PPgMA is observed, which is likely to correspond to the formation of a minor extent of amide groups [27]. This is due to the reaction of secondary amine, reported in Scheme 2, taking place in competition with the reaction of primary amine (Fig. 8, inset).

Grafting was also evaluated by means of size exclusion chromatography (SEC); plots for PPgMA, PPgMA/oib-POSS and PPgMA/am-POSS as obtained by melt blending are reported in Fig. 9. Neat PPgMA shows a monomodal molar mass distribution, centred at *ca.* 90,000 g/mol. On the other hand, the chromatogram for PPgMA/oib-POSS clearly shows a bimodal distribution with the main peak corresponding to PPgMA and an additional peak centred at 810 g/mol, assigned to ungrafted oib-POSS. The chromatogram for PPgMA/am-POSS only shows a very weak signal in the molar mass range corresponding to unbound am-POSS, confirming the high grafting yield on PPgMA.

3.3. Thermal stability

Thermal and thermoxidative stabilities of PPgMA/POSS were studied by means of thermogravimetry in inert (N_2) and oxidative (air) conditions. TGA plots in nitrogen for PPgMA, PPgMA/oib-POSS and PPgMA/am-POSS are reported in Fig. 10. When heating in inert atmosphere, PPgMA undergoes the well-known thermal degradation process for polypropylene [28], starting at *ca.* 300 °C and leading to complete volatilisation. PPgMA/oib-POSS shows an additional mass loss step, starting at *ca.* 200 °C and leading to about 5% mass loss (see inset in Fig. 10), due to POSS evaporation, as observable in Fig. 10 and previously reported [20,29]. On the other hand, no POSS evaporation at low temperature is observed with PPgMA/am-POSS, confirming the extensive grafting of am-POSS. Both oib-POSS and am-POSS slightly increase the temperature for maximum mass loss rate (*ca.* 11 and 15 °C respectively), showing a limited stabilisation of the PPgMA matrix.

When heating in air, oxygen plays an important role in PPgMA degradation, accelerating polymeric chains degradation at low temperatures through peroxidation [28], resulting in lower temperatures for PPgMA volatilisation. The mass loss curve for PPgMA/oib-POSS shows very limited differences as compared to neat PPgMA in terms of both T_{onset} and T_{max}, indicating that non-reactive POSS does not influence the mass loss process in these conditions, namely due to POSS evaporation upon heating (Fig. 11), which occurs in competition with POSS ceramisation [29]. In contrast, grafted am-POSS clearly improves the oxidative stability, despite am-POSS and oib-POSS show similar behaviour upon heating (Fig. 11). Indeed, the mass loss rate for PPgMA/am-POSS is considerably lower as compared to neat PPgMA in the range from 250 to 350 °C, showing an increase in T_{max} (*ca.* 40 °C) and resulting in an overall delayed mass loss in TGA. The higher stability towards thermoxidative degradation is explained by the accumulation of POSS on the sample surface during the earlier stage of PPgMA/am-

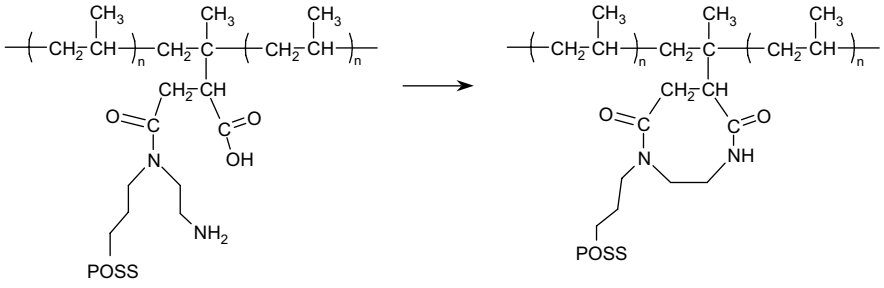

Scheme 2. Amino POSS reaction on MA producing amide groups.

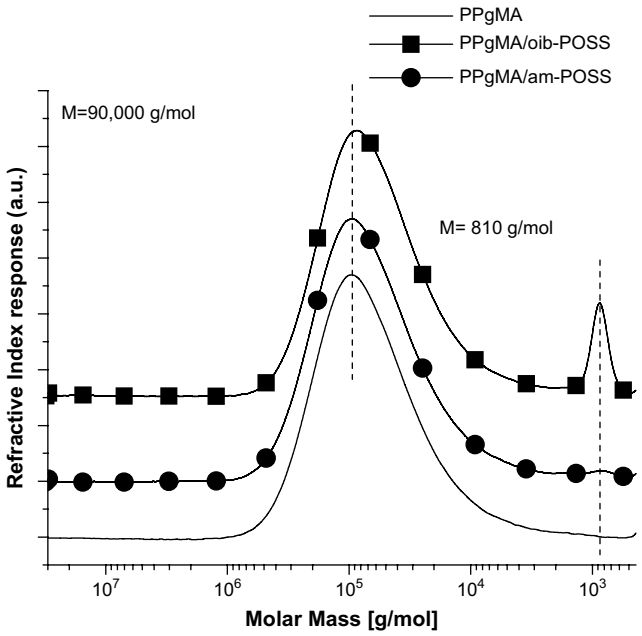

Fig. 9. SEC plots for PPgMA, PPgMA/oib-POSS and PPgMA/am-POSS as obtained by melt blending (curves shifted for clarity).

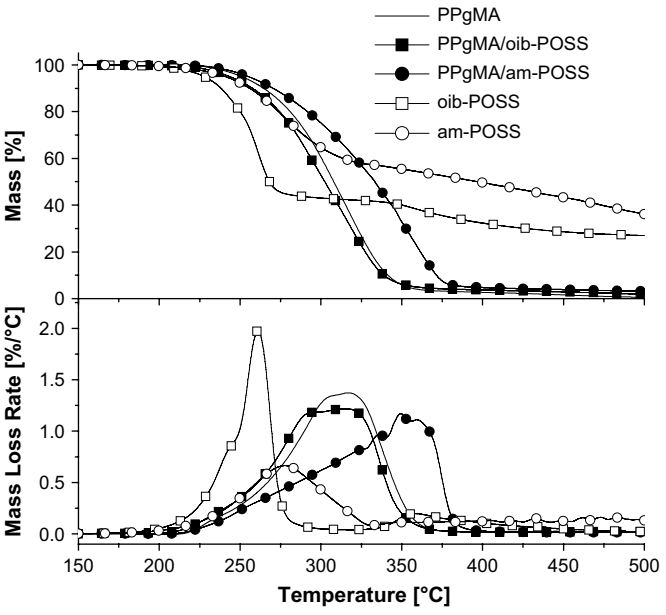

Fig. 11. TGA plots in air for PPgMA/oib-POSS and PPgMA/am-POSS compared to neat PPgMA, oib-POSS and am-POSS.

POSS degradation. Indeed, volatilisation of grafted POSS is hindered as compared to unbound oib-POSS, allowing POSS oxidation with the production of a ceramic phase [29] which acts as a protective barrier, limiting the polymer volatilisation rate.

Further evidence on the role of am-POSS on thermoxidative degradation of the polymeric matrix can be given by monitoring the mass loss in air in isothermal conditions at 250 °C, which corresponds to the beginning of the degradation of the pure matrix (Fig. 12).

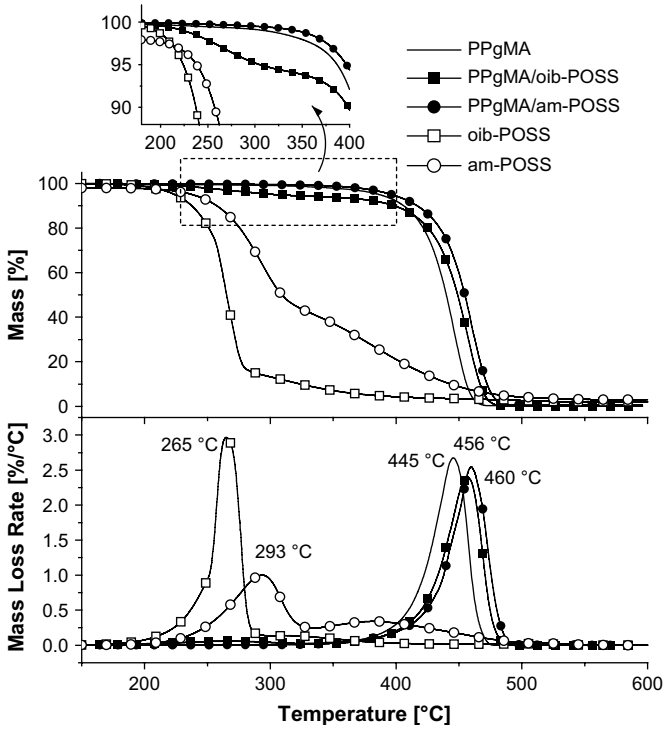

Fig. 10. TGA plots in nitrogen for PPgMA/oib-POSS and PPgMA/am-POSS compared to neat PPgMA, oib-POSS and am-POSS.

Neat PP gives a rapid degradation, showing 50% mass loss after 20 min and leading to a stable 6% residue after 300 min. A similar behaviour is observed with PPgMA/oib-POSS, showing 50% mass loss after 23 min and a slightly higher stable residue (9%) after 300 min. The limited modification of PPgMA thermoxidative degradation kinetics brought by oib-POSS is related to the partial formation of a ceramic phase through POSS thermoxidation in isothermal condition. Indeed, at 250 °C oib-POSS undergoes evaporation in competition with oxidation, leading to an insoluble glassy phase, as previously reported [30]. A significantly slower mass loss rate is obtained for PPgMA/am-POSS, showing 50% mass loss after 45 min and leading to a 15% residue after 300 min. In this case, POSS is retained in the condensed phase thanks to grafting, resulting in accumulation of a ceramic physical barrier by POSS thermoxidation. This accounts for the slower weight loss kinetics and the higher residue compared to PPgMA/oib-POSS.

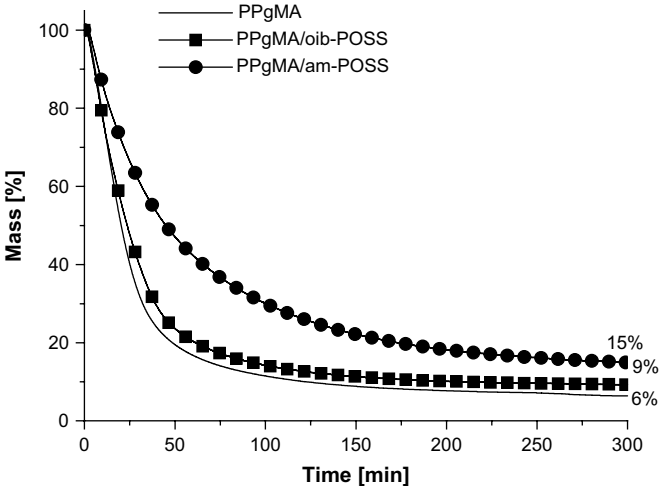

Fig. 12. Isothermal TGA plots in air for PPgMA/oib-POSS and PPgMA/am-POSS compared to neat PPgMA.

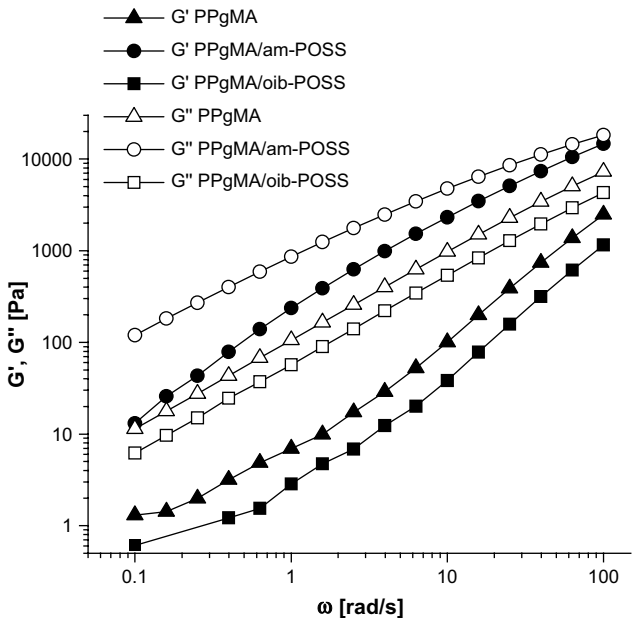

Fig. 13. G' and G'' plots for PPgMA/oib-POSS and PPgMA/am-POSS compared to PPgMA.

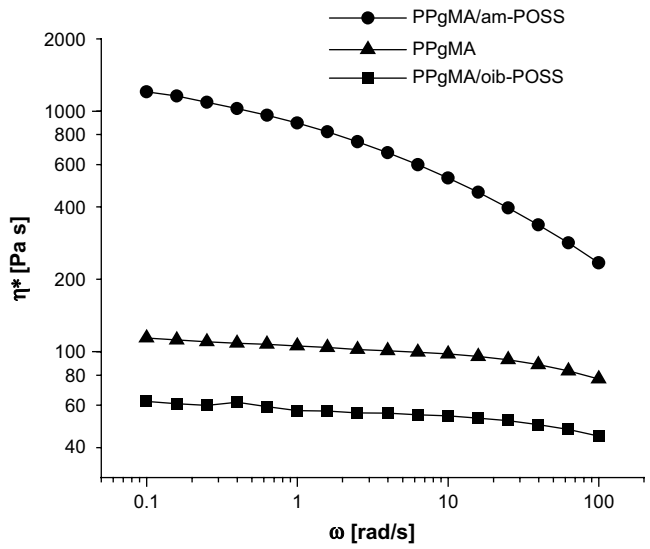

Fig. 14. Complex viscosity plot for PPgMA/oib-POSS and PPgMA/am-POSS compared to PPgMA.

3.4. Rheology

In Fig. 13 elastic (G') and loss (G'') modulus *vs.* frequency for PPgMA, PPgMA/oib-POSS and PPgMA/am-POSS as obtained after melt blending are reported. Both G' and G'' show lower values for PPgMA/oib-POSS as compared to neat PPgMA, owing to plasticization by oib-POSS, whereas dramatic increases are obtained for PPgMA/am-POSS. G' plots do not show low frequency plateau in the explored frequency range, evidencing no solid-like behaviour, neither for PPgMA/oib-POSS nor for PPgMA/am-POSS, most likely because of the low POSS content. Indeed, in the literature POSS/POSS interactions determining solid-like behaviour have been reported but only for significantly higher POSS loadings, with both tethered and untethered POSSs. For example, in PS/POSS copolymers, solid-like behaviour was reported only for POSS loadings $\geq$ 42%wt. [31] Whereas, for untethered POSS, solid-like behaviour at low frequency for ethylene–propylene copolymers filled with octamethyl POSS at contents higher than 10%wt. was reported [32].

In Fig. 14 complex viscosity curves *vs.* frequency for PPgMA, PPgMA/oib-POSS and PPgMA/am-POSS as obtained after melt blending are reported. Both PPgMA and PPgMA/oib-POSS show quasi-Newtonian behaviour in the explored frequency range but the presence of oib-POSS induces a lower viscosity as compared to the neat polymer matrix, which is related to a plasticization effect induced by the unbound POSS. This is in agreement with results previously reported for PMMA/oib-POSS blends, showing zero-shear-rate viscosity reductions at POSS loadings $\leq$5%vol., explained by the free volume increase due to isobutyl groups mobility [33]. On the other hand, the complex viscosity of PPgMA/ma-POSS is approximately one order of magnitude higher than that of PPgMA and shows a significant shear thinning behaviour induced by the presence of am-POSS. This increase in complex viscosity is in agreement with results on POSS-grafted poly(styrene-*co*-diphenylphosphine oxide) by Lee et al. [34], whereas other authors reported a decrease in zero-shear-rate viscosity for both PS/POSS [31] and PMMA/POSS copolymers [33].

The dramatic effects brought by am-POSS to PPgMA melt behaviour are most likely related to the strong interactions occurring between POSS-grafted chains, affecting their mobility in the polymer melt. Various models have been proposed to explain modifications of macromolecules dynamics in the presence of POSS, including sticky reptation and association effects [35,36,31–33], inertial effects [31] and particle-to-particle interactions [32].

Considered the low grafted POSS concentration (less than one POSS per 400 propylene units) and the presence of a small amount of unreacted POSS, the most compelling explanation for the results discussed here is based on the model proposed by Kopesky et al. [33]: POSS grafted on PPgMA chains associates with clusters of untethered POSS, which acts as sticky points hindering macromolecular reptation. The detachment of stickers requires additional energy, resulting in higher viscosity and modulus as compared to PPgMA.

3.5. Mechanical properties

The Young's modulus (E), yield stress (σ_y) and elongation at break (Δl) measured through uniaxial tensile tests on PPgMA/POSS are reported in Table 1 and compared to neat PPgMA. The crystallinity (X_c) for all the tested materials was also measured by DSC to correlate with mechanical properties, showing a slightly lower crystallinity for both PPgMA/am-POSS and PPgMA/oib-POSS.

The addition of oib-POSS results in a drop in PPgMA stiffness in terms of lower elastic modulus (15%) and yield stress (21% on σ_y), whereas elongation at break is increased (6%), resulting in an overall reduction in mechanical performances as compared to neat PPgMA. This is in agreement with findings from a previous study on the mechanical properties of PP/oib-POSS, which showed a reduction of both Young's modulus and yield stress at POSS loadings lower than 10%wt. [37].

This negative effect on mechanical properties brought by oib-POSS gives even more prominence to the results obtained for PPgMA/am-POSS which shows a significant increase in Young's modulus (38%) and yield stress (32%) as compared to PPgMA. It is worth noticing that this increase in stiffness cannot be attributed to

Table 1
Tensile tests' results

	E [GPa]	σ_y [MPa]	$\Delta l/l_0$ [%]	X_c [%]
PPgMA	1.30 ± 0.05	25.3 ± 1.4	645 ± 23	47.0
PPgMA/am-POSS	1.80 ± 0.10	33.4 ± 0.6	423 ± 32	45.0
PPgMA/oib-POSS	1.10 ± 0.10	19.9 ± 0.6	686 ± 27	43.9

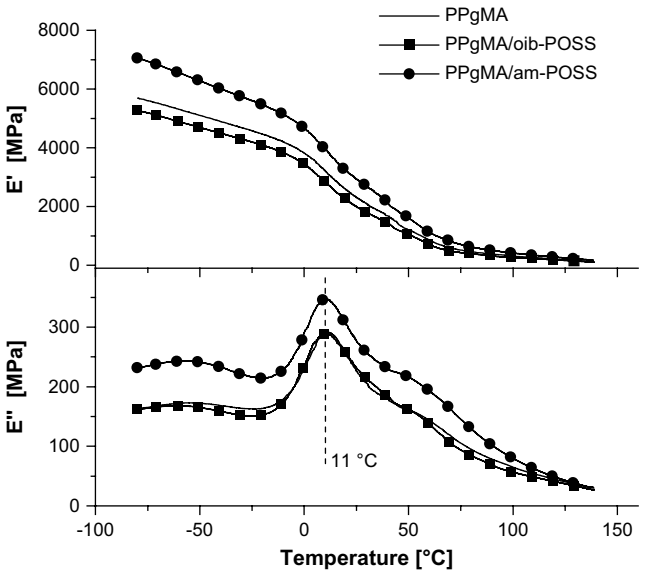

Fig. 15. Storage (E') and loss modulus (E'') plots for PPgMA/oib-POSS and PPgMA/am-POSS compared to PPgMA.

a change in crystallinity, since a reduction in X_c, like that shown in Table 1, usually results in stiffness reduction. On the other hand, the elongation at break for PPgMA/am-POSS is significantly reduced as compared to the reference PPgMA, suggesting a lower toughness for the POSS-grafted system.

Further investigation on mechanical properties was carried out by Dynamic Mechanical Thermal Analysis (DMTA). The spectra for storage modulus (E'), loss modulus (E'') and tan δ for PPgMA/oib-POSS and PPgMA/am-POSS compared to PPgMA are reported in Fig. 15. All three materials clearly show the α-relaxation process corresponding to the glass transition of PPgMA macromolecules. No significant differences in terms of α-relaxation temperature are obtained for PPgMA/oib-POSS and PPgMA/am-POSS compared to neat PPgMA, all three materials showing a peak of E'' at 11 °C. On the other hand, storage modulus is strongly affected by POSS molecules. The presence of unbound oib-POSS results in a decrease of the storage modulus of about 10% over the whole temperature range, in agreement with the softening effect observed in uniaxial tensile tests, whereas only minor changes are shown in the loss modulus plot. A clear stiffening effect is induced by the grafted am-POSS molecules, as shown by the increase of loss and storage modulus (about +25%) over the whole temperature range.

The reported improvements in stiffness obtained for PPgMA/am-POSS as compared to the reference polymer suggest the modification of macromolecules mobility during deformation, due to the presence of POSS grafted onto PPgMA chains. Given that grafted POSS can aggregate with each other to form nanoclusters, as evidenced by XRD and TEM analyses, it is proposed that these nanoclusters lead to a partial physical crosslinking between adjacent PPgMA chains, thus affecting macromolecular relaxation under stress.

4. Conclusions

The preparation of a PPgMA/POSS hybrid was obtained by one-step reactive melt blending.

Morphological analyses on this hybrid showed POSS dispersion at the nanoscale, whereas the corresponding nanocomposite (obtained by the use of non-reactive POSS) contains residual micron-sized aggregates when processed in the same conditions.

The reaction efficiency was assessed, showing a high reaction yield. The chemical reactivity between POSS and PPgMA is therefore the key factor for nanofiller dispersion.

The presence of POSS moieties grafted on PPgMA was found to improve thermoxidative stability, in terms of delayed mass loss during thermal degradation under air, as compared to both neat PPgMA and PPgMA containing the correspondent non-reactive POSS.

POSS grafting on PPgMA chains was shown to radically affect the molecular mobility, resulting in a higher melt viscosity and, more interestingly, in a significant stiffness and strength increase. The effect of grafted POSS on molecular mobility is explained by POSS/POSS interactions to form nanoclusters that can behave as physical crosslink points for the unfolding of PPgMA chains under deformation.

Acknowledgements

This study was carried out in the frame STRP European research program "NANOFIRE", no. 505637, in the sixth Framework Program.

The authors are grateful to Mr. Emiliano Bilotti from Queen Mary, University of London (UK), for his precious contribution to the specimen preparation and mechanical testing as well as to Mr. Claudio Uliana from Department of Chemistry and Industrial Chemistry of Genoa University (I) for TEM analyses.

References

[1] Konig C, Van Duin M, Pagnoulle C, Jerome R. Prog Polym Sci 1998;23(4):707–57.
[2] Hu GH, Sun YJ, Lambla MJ. J Appl Polym Sci 1996;61(6):1039–47.
[3] Bhattacharya A, Misra BN. Prog Polym Sci 2004;29(8):767–814.
[4] Moad G. Prog Polym Sci 1999;24(1):81–142.
[5] Bettini SHP, Agnelli JAM. J Appl Polym Sci 1999;74(2):247–55.
[6] Passaglia E, Coiai S, Aglietto M, Ruggeri G, Rubertà M, Ciardelli F. Macromol Symp 2003;198:147–59.
[7] Huang H, Liu NC. J Appl Polym Sci 1998;67(12):1957–63.
[8] Boyer C, Boutevin B, Robin J. Polym Degrad Stab 2005;90(2):326–39.
[9] Harrison PG. J Organomet Chem 1997;542(2):141–83.
[10] Baney RH, Itoh M, Sakakibara A, Suzuki T. Chem Rev 1995;95(5):1409–30.
[11] Voronkov MG, Lavrent'yev VI. Top Curr Chem 1982;102:199–236.
[12] Sanchez C, Soler-Illia GJ, Ribot F, Lalot T, Mayer CR, Cabuil V. Chem Mater 2001;13(10):3061–83.
[13] Kickelbick G. Prog Polym Sci 2003;28(1):83–114.
[14] Kickelbick G. Introduction to hybrid materials. In: Kickelbick G, editor. Hybrid materials, synthesis, characterisation and applications. Weinheim: Wiley-VCH Verlag; 2007. p. 1–48.
[15] Li G, Wang L, Ni H, Pittman Jr CU. J Inorg Organomet Polym 2001;11(3):123–54 and references therein.
[16] Pittman CU, Li G-Z, Ni H. Macromol Symp 2003;196:301–25.
[17] Phillips SH, Haddad TS, Tomczak SJ. Curr Opin Solid State Mater Sci 2004;8(1):21–9.
[18] Seurer B, Coughlin EB. Macromol Chem Phys 2008;209(12):1198–209.
[19] Zhou Z, Zhang Y, Zhang Y, Yin N. J Polym Sci Part B Polym Phys 2008;46(5):526–33.
[20] Fina A, Tabuani D, Frache A, Camino G. Polymer 2005;46(19):7855–66.
[21] Fu BX, Yang L, Somani RH, Zong SX, Hsiao BS, Philips S, et al. J Polym Sci Part B Polym Phys 2001;39(22):2727–39.
[22] Wunderlich B. Macromolecular physics. In: Crystal melting, vol. 3. New York: Academic Press; 1980 [chapter 7].
[23] ASTM International Standard D638-03.
[24] Khafagy RM, Badr YA. J Polym Sci Part B Polym Phys 2005;43(20):2829–42.
[25] Lotz B, Wittmann JC, Lovinger AJ. Polymer 1996;37(22):4979–92.
[26] Phillips RA, Wolkowicz MD. In: Moore Jr EP, editor. Polypropylene handbook. Munich: Hanser Publishers; 1996. p. 113–76.
[27] Socrates G. Infrared and Raman characteristics group frequencies. Chichester: John Wiley and Sons, LTD; 2001 [chapter 10].
[28] Grassie N, Scott G. Polymer degradation and stabilization. Cambridge: Cambridge University Press; 1985 [chapter 2].
[29] Fina A, Tabuani D, Carniato F, Frache A, Boccaleri E, Camino G. Thermochim Acta 2006;440(1):36–42.
[30] Fina A, Tabuani D, Frache A, Boccaleri E, Camino G. Isobutyl POSS thermal degradation. In: Le Bras M, Wilkie C, Bourbigot S, editors. Fire retardancy of polymers: new applications of mineral fillers. Cambridge, UK: Royal Society of Chemistry; 2005. p. 202–20.
[31] Romo-Uribe A, Mather PT, Haddad TS, Lichtenhan JDJ. J Polym Sci Part B Polym Phys 1998;36(11):1857–72.

[32] Fu BX, Gelfer MY, Hsiao BS, Phillips S, Viers B, Blansky R, et al. Polymer 2003;44(5):1499–506.
[33] Kopesky ET, Haddad TS, Cohen RE, McKinley GH. Macromolecules 2004;37(24):8992–9004.
[34] Lee A, Xiao J, Feher FJ. Macromolecules 2005;38(2):438–44.
[35] Leibler L, Rubinstein M, Colby RH. Macromolecules 1991;24(16):4701–7.
[36] Wientjes RHW, Jongschaap RJJ, Duits MHG, Mellema J. J Rheol 1999; 43(2):375–91.
[37] Baldi F, Bignotti F, Fina A, Tabuani D, Riccò T. J Appl Polym Sci 2007;105(2):935–43.